FISEVIER

Contents lists available at ScienceDirect

Journal of the Mechanical Behavior of Biomedical Materials

Journal of the Mechanical Behavior of Biomedical Materials

journal homepage: www.elsevier.com/locate/jmbbm



Non-enzymatic glycation of annulus fibrosus alters tissue-level failure mechanics in tension

Benjamin Werbner^a, Matthew Lee^a, Allan Lee^b, Linda Yang^b, Mohamed Habib^{c,d}, Aaron J. Fields^c, Grace D. O'Connell^{a,c,*}

- ^a Department of Mechanical Engineering University of California, Berkeley, USA
- ^b Department of Bioengineering University of California, Berkeley, USA
- ^c Department of Orthopaedic Surgery University of California, San Francisco, USA
- ^d Mechanical Engineering Department Al Azhar University, Cairo, Egypt

ARTICLE INFO

Keywords: Advanced glycation end products Annulus fibrosus Intervertebral disc Tissue failure mechanics Diabetes Aging

ABSTRACT

Advanced-glycation end products (AGEs) are known to accumulate in biological tissues with age and at an accelerated rate in patients with diabetes and chronic kidney disease. Clinically, diabetes has been linked to increased frequency and severity of back pain, accelerated disc degeneration, and an increased risk of disc herniation. Despite significant clinical evidence suggesting that diabetes-induced AGEs may play a role in intervertebral disc failure and substantial previous work investigating the effects of AGEs on bone, cartilage, and tendon mechanics, the effects of AGEs on annulus fibrosus (AF) failure mechanics have not yet been reported. Thus, the aim of this study was to determine the relationship between physiological levels of AGEs and AF tensile mechanics at two distinct loading rates. *In vitro* glycation treatments with methylglyoxal were applied to minimize changes in tissue hydration and induce two distinct levels of AGEs based on values measured from human AF tissues.

In vitro glycation increased modulus by 48–99% and failure stress by 45–104% versus control and decreased post-failure energy absorption capacity by 15–32% versus control (ANOVA p < 0.0001 on means; range given across two loading rates and glycation levels). AGE content correlated strongly with modulus (R = 0.74, p < 0.0001) and failure stress (R = 0.70, p < 0.0001) and moderately with post-failure energy absorption capacity (R = 0.62, p < 0.0001). Failure strain was reduced by 10–17% at the high-glycation level (ANOVA p = 0.01). Tissue water content remained near or just above fresh-tissue levels for all groups. The alterations in mechanics with glycation reported here are consistent with trends from other connective tissues but do not fully explain the clinical predisposition of diabetics to disc herniation. The results from this study may be used in the development of advanced computational models that aim to study disc disease progression and to provide a deeper understanding of altered structure-function relationships that may lead to tissue dysfunction and failure with aging and disease.

1. Introduction

Fiber-reinforced tissues of the musculoskeletal system, such as the annulus fibrosus (AF) in the intervertebral disc, experience large, complex loads during daily activities. Repetitive or excessive loading may initiate structural damage and lead to mechanical failure, causing debilitating pain and reduced mobility (Buckwalter, 1995; Luoma et al., 2000). Additionally, disc tissue structure and composition change with age and disease, which alters mechanical behavior and may predispose

the disc and surrounding structures to damage (Urban and Roberts, 2003; Adams and Roughley, 2006). Thus, it is essential to comprehensively characterize tissue structure-function relationships and failure mechanisms to better understand and prevent avoidable injuries, including those occurring due to age and disease (O'Connell et al., 2015).

In addition to the natural aging process, several clinical conditions have been linked to accelerated degeneration and herniation of the intervertebral disc. Among cardiovascular risk factors studied in the

^{*} Corresponding author. 5122 Etcheverry Hall, #1740, Berkeley, CA, 94720-1740, USA. *E-mail address*: g.oconnell@berkeley.edu (G.D. O'Connell).

Nurses' Health Study, diabetes had the highest relative risk of intervertebral disc herniation (relative risk: 1.52, 95% CI: 1.17 to 1.98) after correcting for additional risk factors such as age, body mass index, level of exercise, and several other important factors (Jhawar et al., 2006). Additionally, previous work showed that diabetes was associated with increased frequency and severity of lower back pain and diminished treatment outcomes (Mäntyselkä et al., 2008; Licciardone et al., 2013; Takahashi et al., 2013; Freedman et al., 2011). Approximately 10.5% of Americans are diabetic and with 1.5 million new cases diagnosed every year and total annual costs estimated at \$327 billion, diabetes and the associated complications represent one of the most significant healthcare issues in the United States (CDC, 2020).

One of the most well-documented changes in connective tissues occurring with diabetes is the accumulation of advanced glycation endproducts (AGEs) (Monnier et al., 1986; Singh et al., 2001; Vlassara and Palace, 2002; Ahmed, 2005; Tsai et al., 2014). Research in this group of post-translational protein crosslinks and adducts has grown in recent years, as they exhibit a wide range of chemical, cellular, and tissue-level effects that have been strongly implicated in diabetes-related complications (Singh et al., 2001; Vlassara and Palace, 2002; Ahmed, 2005). Minimal biological turnover and a long half-life makes collagen and proteoglycans in the intervertebral disc particularly susceptible to interaction with glycating metabolites and AGE formation (Pokharna and Phillips, 1998; Vlassara and Palace, 2002; Snedeker and Gautieri, 2014). AGEs have also been shown to accumulate naturally in the disc with age (Pokharna and Phillips, 1998; Sivan et al., 2006), although the rate and extent of intradiscal AGE accumulation is amplified with diabetes (Tsai et al., 2014).

Previous studies of soft tissues in the musculoskeletal system, such as articular cartilage, tendon, and the intervertebral disc, have probed the effects of AGEs on tissue mechanics using animal models of diabetes or in vitro crosslinking with ribose or methylglyoxal (MGO) (Reddy et al., 2002; Verzijl et al., 2002; Reddy, 2004; Wagner et al., 2006; de Oliveira et al., 2011; Fox et al., 2011; Li et al., 2013; Jazini et al., 2012; Gautieri et al., 2017; Svensson et al., 2018). More recently, studies have also begun to investigate structural and functional effects of controlled in vivo AGE accumulation through animal models fed AGE-rich diets (Illien--Jünger et al., 2015; Krishnamoorthy et al., 2018; Hoy et al., 2020). These studies reported noteworthy alterations to tissue structure and function across multiple length scales. The most widely reported alterations to connective tissue mechanics include increased tissue stiffness, failure strength, energetic toughness, and reduced viscoelasticity (Reddy et al., 2002; Verzijl et al., 2002; Reddy, 2004; Wagner et al., 2006; Li et al., 2013; Snedeker and Gautieri, 2014; Gautieri et al., 2017; Svensson et al., 2018). However, a few studies in diabetic animals have reported decreases in tissue stiffness (de Oliveira et al., 2011; Fox et al., 2011). Additional studies have also observed significant changes in disc-adjacent tissues, such as vertebral bodies and endplates, which are known to play an important role in load-distribution and nutrient transport (Viguet-Carrin et al., 2006; Fields et al., 2015; Illien-Jünger et al., 2015, 2016; Acevedo et al., 2018; Dolor et al., 2019; Zhou et al., 2021).

Despite these advances, the effects of AGEs on AF tensile failure mechanics have not yet been reported. Additionally, *in vitro* soak treatments applied in previous studies tend to cause tissue swelling, which is known to alter tissue mechanics and potentially confound mechanical testing results (Han et al., 2012; Bezci et al., 2015; Safa et al., 2017; Werbner et al., 2019; Werbner et al., 2021). Thus, the specific aim of this study was to quantify the relationship between physiological, glycation-induced biochemical changes and AF tensile failure mechanics while maintaining physiological tissue hydration levels. The broader aim of this study was to provide a more complete understanding of mechanisms that may help explain the increased propensity for disc degeneration and herniation with diabetes. Thus, the current study evaluated pre-failure, failure, and post-failure properties of normal and *in vitro* glycated bovine caudal AF tissue by comparing

measured mechanics between control, moderate glycation, and high glycation groups, and by correlating biochemical composition, including AGE content, to mechanical properties at two distinct loading rates. Furthermore, human cadaver AF tissue from a cross-sectional population of donors of both sexes and a range of ages was assayed to provide a physiologically relevant range of AGEs in adult humans as a target for *in vitro* glycation.

2. Methods

Fresh bovine coccygeal spine sections were acquired from a local abattoir (n=19, age 18–24 months). Bovine discs were used to investigate AF mechanics due to their larger disc area and similarities in biochemical and mechanical properties to healthy human discs (O'Connell et al., 2007; Demers et al., 2004; Beckstein et al., 2008). Musculature was removed from the spine and discs were dissected from levels CC2-CC5. Rectangular specimens 2 mm thick and 5 mm wide were prepared from the middle-outer region of the anterior and posterior AF using a freezing stage microtome and oriented with the length along the circumferential direction and the width along the axial direction (Fig. 1A). Preliminary work ensured no differences in mechanics between anterior and posterior bovine AF (n=6/group, Student's p>0.3).

A full-width, half-depth notch was created using a custom cutting jig that ensured 1 mm thickness at the midlength; the width of the notch area was then further reduced to 1.25 mm using another custom cutting jig (Fig. 1B). A similar notch geometry was previously developed and validated by our lab using a combined experimental and computational approach to ensure tissue failure properties were robustly and consistently measured (Werbner et al., 2017). Previous studies reported no significant differences in stiffness or strength between notched and intact fiber-reinforced soft-tissues, suggesting a limited effect of stress concentrations at the notch site (Taylor et al., 2012; Von Forell et al., 2014).

Preliminary work was conducted to determine the appropriate concentration and soak temperature of the glycation solution to achieve two distinct, physiologically relevant levels of AGEs. The range of physiological AGE concentrations was determined by assaying the AGE content of unfixed human lumbar AF tissues obtained from 10 cadaveric spines (Table 1; mean age 58.4 \pm 9.4 years; IRB exempt - Category 4). Briefly, 36 AF specimens were dissected, lyophilized, digested in papain, hydrolyzed in 6N HCl at 120 °C, neutralized, and assayed for total fluorescence using a quinine sulfate standard at excitation/emission wavelengths of 370 nm/440 nm to estimate total AGE content.

Bovine AF samples in the control group (CTL, n = 26) were soaked for 18 h at 25 °C in 10 mL of a solution containing 5% phosphatebuffered saline (PBS) and 5%w/v polyethylene glycol (PEG) pHbalanced to 7.4. Previous studies found that this solution avoided excessive tissue swelling caused by traditional 0.9% PBS treatments as well as excessive solute deposition caused by hyperosmotic saline solutions (Safa et al., 2017; Werbner et al., 2019; Bezci et al., 2020; Bloom et al., 2021; Werbner et al., 2021). Based on the human data from our preliminary work, glycated specimens were soaked in 0.3 M methylglyoxal pH-balanced to 7.4 at either 25 °C or 50 °C for 18 h immediately prior to testing (GLY25 (n = 26) and GLY50 (n = 26), respectively). Previous work from our lab analyzed the thermal profile of bovine annulus fibrosus tissue using differential scanning calorimetry and did not observe any measurable deviations in the trace until 65-70 °C, consistent with previous studies of similar connective tissues (Domán and Illés, 2004; Bálint et al., 2009; Chae et al., 2009; Samouillan et al., 2011). Thus, it was assumed that incubation at 50 $^{\circ}$ C did not affect the bulk tissue composition or mechanical response.

Specimens were gripped for mechanical testing using custom-made, serrated screw-clamp grips. Specimens were tested in a custom-built water bath containing the previously mentioned PBS-PEG mixture to maintain tissue hydration during testing (total testing time up to 150 min for low-rate testing). A monotonic 0.1 N preload was applied to

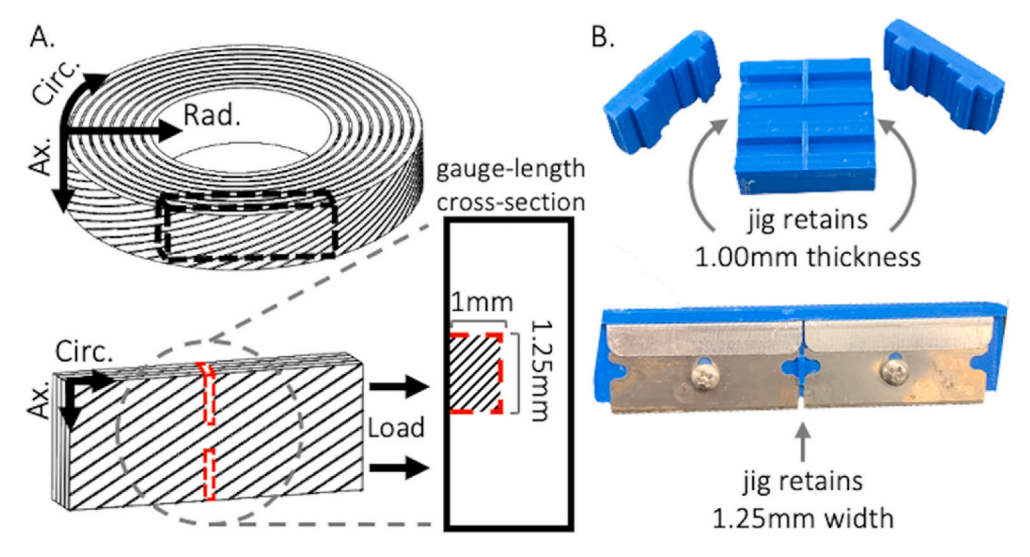


Fig. 1. (A) Disc schematic showing circumferential-axial specimen orientation and loading direction. Inset shows reduced cross-sectional area at the midlength, which was notched to ensure repeatable failure. (B) Custom cutting jigs used to ensure that the tissue remaining at the notch site had repeatable dimensions of 1×1.25 mm

Table 1
Human tissue donor information and disc AGE contents.

Donor Age	Donor Sex	Donor BMI	Disc Level	Disc Grade	AGE Content (ngQ/ mgDW)
38	Male	27	L4-	III	422.23
			L5		
			L5-	III	437.62
			S1		
52	Male	25	L3-	III	452.96
			L4		
55	Male	26	L3-	II	416.57
			L4		
			L4-	II	459.40
			L5		
56	Male	23	L3-	II	432.65
			L4		
57	Male	29	L4-	IV	647.32
			L5		
64	Male	16	L3-	III	503.87
			L4		
	Female	31	L3-	III	507.26
			L4		
			L4-	III	598.57
			L5		
63	Female	25	L2-	IV	410.83
			L3		
			L4-	IV	416.41
	n 1	00	L5	***	560.50
66	Female	22	L3-	III	562.58
			L4	***	FF1 00
			L4-	III	551.23
73	P1	0.4	L5	***	F06.6F
	Female	24	L3-	III	506.65
			L4	***	(00.00
			L4-	III	629.29
			L5		

remove slack from the tissue. Cyclic preconditioning was not applied to avoid altering pre-testing tissue water content, which could affect treatment groups differently (Schmidt et al., 2016). Scale bar photographs were taken to measure sample-specific length (9.90 \pm 2.03 mm). Uniaxial tension was applied monotonically along the circumferential direction at either a low (0.1 mm/min, 0.017%/sec, 'Lo') or high (50 mm/min, 8.33%/sec, 'Hi') loading rate until the specimen separated into two pieces with no load-bearing components between them (end-of-test load threshold = 0.2N). Physiological loading rates

experienced by the AF are complex, varied, and difficult to determine, in part because they are mitigated by a myriad of muscle contractions (White III and Panjabi, 1990). The low and high loading rates used here were selected to be within a reasonable range of physiological loading conditions and to highlight potential rate-sensitive differences in mechanics (Gregory and Callaghan, 2010; Werbner et al., 2019).

Engineering strain was calculated as the measured change in testmachine crosshead displacement divided by the initial gauge length. Engineering stress was calculated as the measured force divided by the initial cross-sectional area at the midlength. The linear-region modulus was calculated using a custom, sequential linear-regression optimization to the stress-strain response to ensure exclusion of the toe- and yieldregions. Failure stress was defined as the maximum stress and failure strain as the corresponding strain. Strain energy density was determined through numerical integration of the engineering stress-strain response. The 'failure energy ratio' was defined as the strain energy density up to the point of failure divided by the total strain energy density (i.e., until the end-of-test load threshold was achieved). While Lagrangian or Eulerian strain descriptions might provide a more accurate characterization of the strain energy density at large deformations, most tissue mechanics studies use the area under the engineering stress-strain curve due to experimental limitations in collecting accurate local deformation data around and beyond bulk failure (Reddy et al., 2002; Reddy, 2004; de Oliveira et al., 2011; Fox et al., 2011; Li et al., 2013; Gautieri et al., 2017). Thus, the engineering stress-strain response was used in this study to facilitate comparison to previous literature.

After mechanical testing, two small tissue samples adjacent to the notch site were removed with a scalpel and weighed before (wet weight, 'WW') and after (dry weight, 'DW') lyophilization to determine water content ('WC', WC = (WW-DW)/WW). Dried specimens were hydrolyzed in 6N HCl at 120 °C for 24 h, after which the HCl solution was allowed to evaporate completely under low heat (40 °C). Lysates were resuspended and assayed for hydroxyproline using the chloramine-T spectrophotometric method (Stegemann and Stalder, 1967). Collagen content ('Col') was calculated assuming a 1:7.5 OHP-to-collagen mass ratio and reported as a percentage of tissue dry weight (mgCol/mgDW) (Hollander et al., 1994). Lysates were also assayed for total fluorescence using a quinine sulfate standard at excitation/emission wavelengths of 370 nm/440 nm. Total fluorescence was reported as equivalent nanograms of quinine normalized by tissue dry weight (ngQ/mgDW) and equivalent micrograms of quinine normalized by tissue collagen content (ugQ/mgCol).

All values are reported as mean \pm standard deviation. A two-way ANOVA on means was performed for all mechanical and biochemical properties (factors = treatment and loading rate); significance for the ANOVA was assumed at p < 0.05. A Tukey HSD post-hoc analysis for multiple pairwise comparisons was performed where significance was found. Significance was assumed at p < 0.05 for the post-hoc analysis. Bivariate linear correlations were established between each pair of biochemical and mechanical properties. Correlation strength was determined based on the correlation coefficient R (weak: |R| < 0.5, moderate: 0.50–0.69, strong: \geq 0.70).

3. Results

All samples exhibited a nonlinear stress-strain response prior to failure and a clear maximum stress corresponding to the initiation of bulk failure (Fig. 2). Mechanical testing data was only included for samples that clearly failed at the midlength (n = 78/84 *i.e.*, 93%).

3.1. Effects of loading rate

For the low-rate control group, the mean linear-region modulus was 27.47 ± 6.60 MPa, failure stress was 11.19 ± 2.36 MPa, failure strain was 0.54 ± 0.07 mm/mm, and failure energy ratio was 0.64 ± 0.10 . For the high-rate control group, the mean linear-region modulus was 38.35 ± 12.42 MPa, failure stress was 14.12 ± 3.66 MPa, failure strain was 0.49 ± 0.09 mm/mm, and failure energy ratio was 0.67 ± 0.10 . Modulus and failure stress increased at the higher loading rate across treatment groups (ANOVA p<0.0002; Fig. 3A–B, light vs dark). In particular, modulus increased 40-44% (HSD p<0.0001) and failure stress increased 9-16% at the higher loading rate (ANOVA p=0.001, HSD p=0.001; Fig. 3A–C). Failure energy ratio was not different between loading rates (ANOVA p=0.84; Fig. 3D).

As only methylglyoxal treatment, and not loading rate, was hypothesized to alter tissue composition, biochemical measurements within treatment groups were pooled between loading rates. The rate-pooled mean water content for the CTL group was 75 \pm 3%/WW, collagen content was 70 \pm 4%/DW, and AGE content was 175 \pm 36 ngQ/mgDW and 250 \pm 54 ugQ/mgCol (Fig. 4).

3.2. Effects of glycation

In vitro glycation had significant effects on pre-failure, failure, and post-failure mechanical properties (Fig. 3). Increasing extent of glycation was associated with higher modulus and failure stress values at both

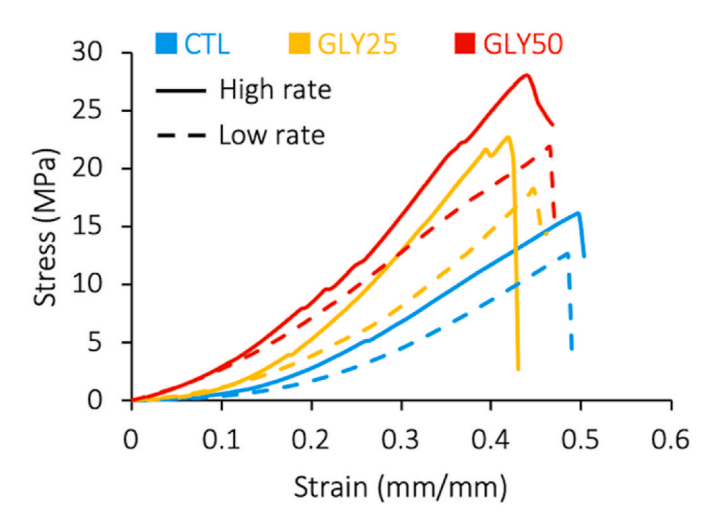


Fig. 2. Representative stress-strain curves for control (CTL) and glycated (GLY25 and GLY50) specimens at the low and high loading rates.

loading rates (ANOVA p < 0.0001; Fig. 3A–B, blue vs orange vs red). In particular, glycation increased mean tensile modulus versus control by 48–94% at the low rate and 53–99% at the high rate (HSD p < 0.0001). Glycation increased failure stress by 45–104% at the low rate and 48–91% at the high rate (HSD p < 0.0001). Glycation decreased failure strain by 10% at the low rate and 17% at the high rate (ANOVA p = 0.02, HSD p = 0.02). Glycation decreased the failure energy ratio by 15–21% at the low rate and 15–35% at the high rate (ANOVA p < 0.0001; HSD p < 0.006).

Biochemical measurements are summarized in Fig. 4. AGE content normalized by dry weight increased 83% and AGE content normalized by collagen content increased 73% in the GLY25 group (ANOVA p < 0.0001, HSD p < 0.0001). AGE content normalized by dry weight increased 236% and AGE content normalized by collagen content increased 222% in the GLY50 group (ANOVA p < 0.0001, HSD p < 0.0001). Water content increased 4% in the GLY50 group versus control (ANOVA p = 0.0008, HSD p = 0.005).

AGE contents for the human AF specimens were normally distributed (Shapiro-Wilk p=0.125) with a mean of 498 \pm 94 ngQ/mgDW; donor-specific values are presented in Table 1.

3.3. Correlations between AGE content and mechanics

AGE content was strongly positively correlated with modulus (R = 0.74, p < 0.0001) and failure stress (R = 0.70, p < 0.0001) (Fig. 5A–B). AGE content was moderately negatively correlated with failure energy ratio (R = -0.62, p < 0.0001) (Fig. 5C). Linear-region modulus was strongly positively correlated with failure stress (R = 0.85, p < 0.0001) (Fig. 5D).

4. Discussion

The specific aim of this study was to determine the relationship between AF advanced glycation end-product content and tissue-level tensile mechanics at two distinct loading rates. *In vitro* glycation treatments were designed to minimize changes in water content and induce two distinct levels of AGEs based on measurements from human cadaver AF tissues (donor age range: 38–73 years). Changes in AF mechanics between glycation groups were reported, as well as correlations between tissue AGE content and mechanics.

In vitro glycation increased linear-region modulus and failure stress at both loading rates (Fig. 3A-B). The increases in mechanical properties were more pronounced at the higher loading rate, which may be attributed to the solid-tissue component having a greater contribution to mechanics at higher loading rates. Increases in modulus and failure stress with glycation are consistent with previous studies that investigated the effects of AGEs on collagenous connective tissue mechanics (Reddy et al., 2002; Verzijl et al., 2002; Reddy, 2004; Wagner et al., 2006; Li et al., 2013; Snedeker and Gautieri, 2014; Gautieri et al., 2017; Svensson et al., 2018). Moreover, increases in modulus and failure stress and decreases in failure strain at the higher loading rate are consistent with first principles of fiber-reinforced triphasic tissues and previous observations of the AF (Gregory and Callaghan, 2010; Werbner et al., 2019). In synthetic materials, an increase in modulus and failure stress generally increases embrittlement. However, despite a concurrent decrease in failure strain, we observed an increase in post-failure energy absorption capacity with glycation (Fig. 3D). This shift in energy absorption may be attributable to non-enzymatic crosslinks between collagen molecules remaining intact after the initiation of bulk failure (Svensson et al., 2013).

In addition to significant group dependent differences in mechanics, we found moderate to strong linear correlations between biochemical and mechanical properties. Specifically, AGE contents were moderately to strongly correlated with tissue mechanics. Additionally, we observed a strong linear correlation between linear-region modulus and failure stress. While previously unpublished for the AF, this has been a

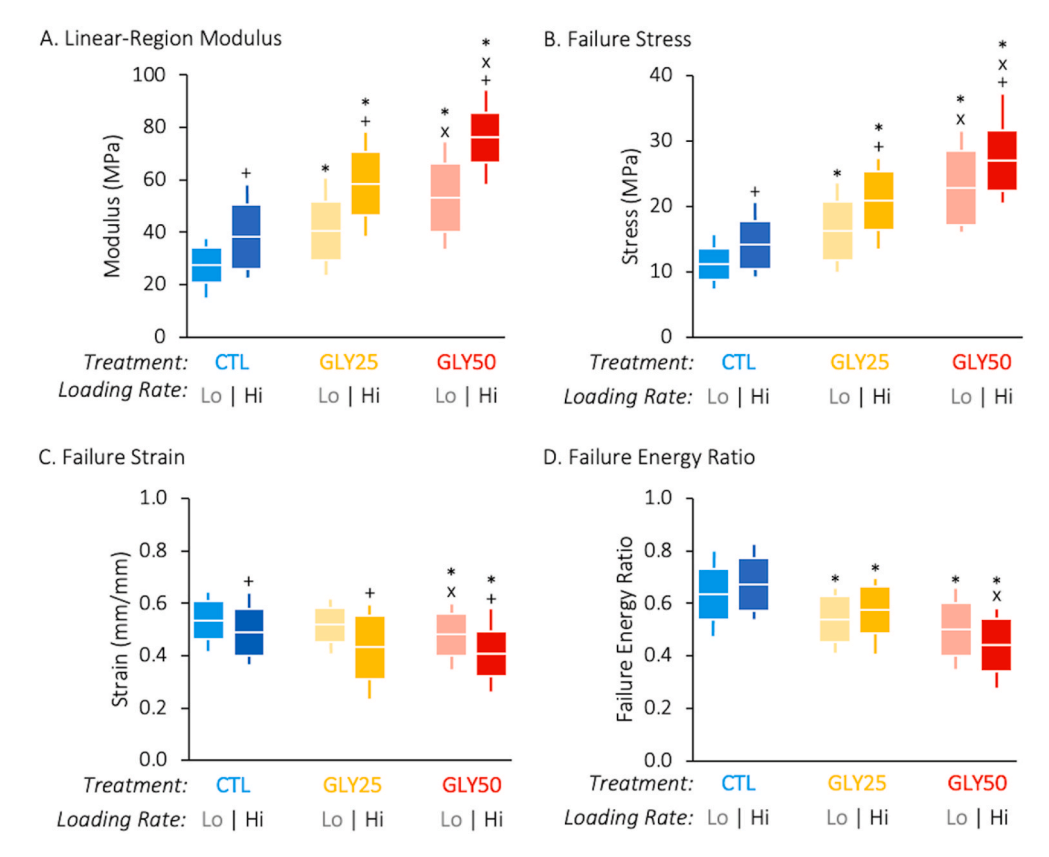


Fig. 3. (A) Linear-region modulus, (B) failure stress, (C) failure strain, and (D) failure energy ratio at each glycation level and loading rate (mean \pm standard deviation \pm range, n=13 per group). Statistics highlight the effect of glycation (* indicates p<0.01 vs CTL and x indicates p<0.01 vs GLY25) and loading rate (+indicates p<0.05 vs Lo).

consistent finding in our work and has significant implications for understanding tissue failure mechanisms. In particular, it may suggest that the rate-dependent mechanical response of connective tissues serves a protective role against failure: failure stress increases proportionately with tissue stiffness, which both increase at higher loading rates associated with potentially traumatic impacts.

While AGE accumulation is known to occur with aging, diabetes, chronic kidney disease (Allen et al., 2015), and AGE-rich diets, there are conflicting reports regarding the impact of in vivo versus in vitro AGE accumulation on soft tissue mechanics. For example, two studies found that tendon stiffness decreased in rats with diabetes induced in vivo (de Oliveira et al., 2011; Fox et al., 2011), in contrast to most in vitro studies that observed increases in stiffness with AGE accumulation (Reddy et al., 2002; Verzijl et al., 2002; Reddy, 2004; Wagner et al., 2006; Li et al., 2013; Snedeker and Gautieri, 2014; Gautieri et al., 2017; Svensson et al., 2018). One limitation of *in vitro* models is that exogenous AGE formation is uncoupled from normal tissue remodeling and adaptation, which may include processes that mitigate the effects of AGE formation (Fields et al., 2015; Illien-Jünger et al., 2016; Dolor et al., 2019). Additionally, it is possible that the specific AGE profile generated from incubation in methylglyoxal differs from that generated from glucose in vivo, which may contribute to the discrepancy between in vivo and in vitro alterations in mechanics with glycation.

While there is a clear clinical predisposition to soft-tissue injury in diabetics, it remains unclear how the changes reported here and elsewhere, namely increased stiffness, strength, and post-failure energy absorption capacity, might predispose diabetic discs to herniation. Despite similar observed alterations in mechanics with glycation, previous investigators have not been able to explain the apparent paradox between increased stiffness and strength without brittleness in labtested tissue and the clinical predisposition of diabetics to connective tissue injury. This may be due to increased stresses experienced by

diabetic patients, altered disc loading conditions, or stress redistribution. It is also possible that the glycated tissue response is anisotropic, with decreases in failure properties in the radial or axial directions (Guerin and Elliott, 2007; O'Connell et al., 2009; Isaacs et al., 2014; Tavakoli et al., 2018; Werbner et al., 2017; Andriotis et al., 2019).

Collagen contents were in the range of previous bovine AF data across treatment groups (Bezci et al., 2019). 18 h in 0.3M methylglyoxal at 25 $^{\circ}\text{C}$ and 50 $^{\circ}\text{C}$ were found to be sufficient for inducing distinct levels of AGEs that were comparable to the human AF tissues measured in this study. The AGE content of the bovine control in this study is likely lower than adult human AGE levels, highlighting the benefit of animal models to provide a wider range of biochemical parameters. Normalizing total fluorescence measurements by tissue dry weight helped promote a clear comparison between species with different amounts of collagen and proteoglycans (Showalter et al., 2012; Bezci et al., 2019). Tissue water contents remained near or just above values reported for fresh tissue, which is a significant improvement from previous studies using 0.15 M saline (Isaacs et al., 2014; Bezci et al., 2019; Werbner et al., 2019; Bezci et al., 2020). Our recent work determined the composition and concentration of buffer needed to minimize AF tissue swelling and solute deposition during the treatment process (i.e., 18-h soak period) (Werbner et al., 2021). This approach was largely successful in maintaining fresh tissue hydration levels, as the mean water content across all groups in this study was 76 \pm 4%, which was only slightly higher than values for fresh bovine tissue reported by Bezci et al., (2019) (74 \pm 5%). The slightly elevated water content in the MGO50 group (4% higher than control) is likely due to greater fluid diffusion into tissue at 50 °C and not due to non-enzymatic crosslinking, as Jazini et al. (2012) noted a decrease in AF water content with increasing glycation.

Preserving fresh-tissue hydration conditions makes comparisons to previous studies more complicated, as they have largely used 0.15 M PBS as a buffer solution during testing. Previous studies showed that

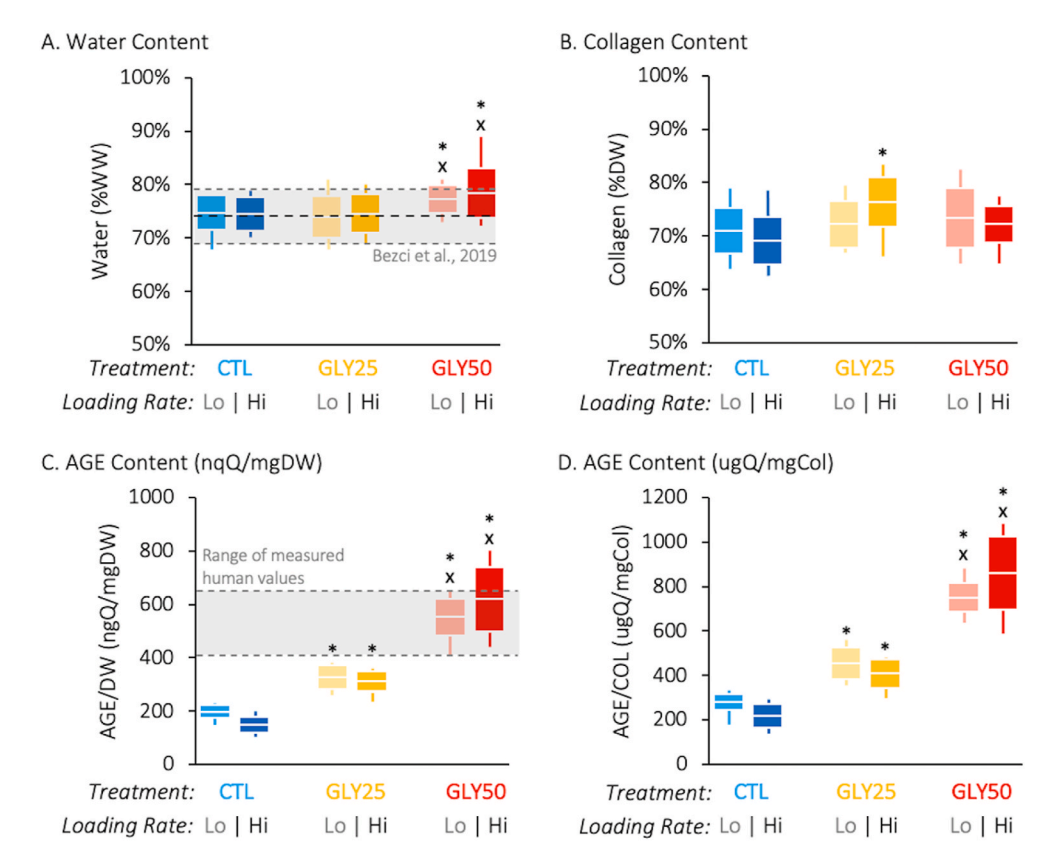


Fig. 4. (A) Water content, (B) collagen content, and (C–D) AGE content at each glycation level and loading rate (mean \pm standard deviation \pm range, n = 13 per group). Fresh AF water content level (mean \pm standard deviation) from Bezci et al. (2019) shown for reference in (A). Range of human AF AGE levels measured in the current study shown for reference in (C). * indicates p < 0.05 vs CTL and x indicates p < 0.05 vs GLY25.

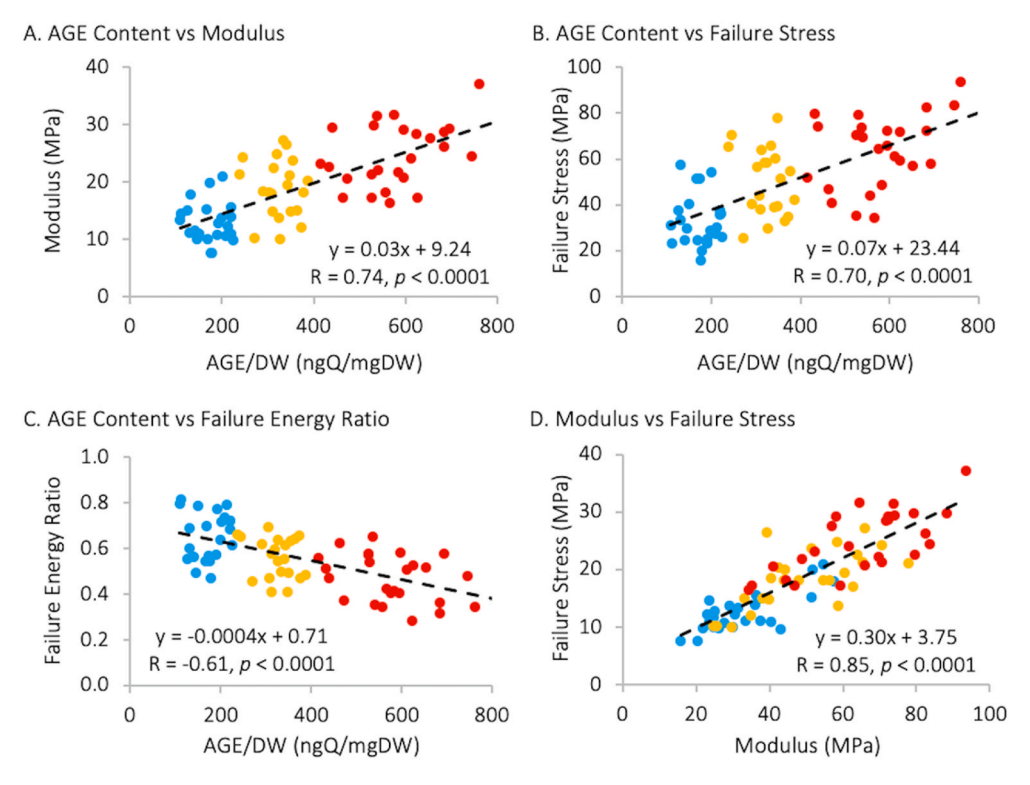


Fig. 5. (A–C) Bivariate linear correlations between AGE content and measured mechanics. (D) Bivariate linear correlation between linear-region modulus and failure stress. Colors indicate rate-pooled glycation treatment groups.

prolonged exposure of tissue samples to 0.15 M PBS significantly increases water content (Galante, 1967; Acaroglu et al., 1995; Ebara et al., 1996; Werbner et al., 2019; Bezci et al., 2020) and may lower modulus by over 80% (Han et al., 2012; Werbner et al., 2019; Werbner et al., 2021). This in part explains why the modulus values reported here are significantly higher than many values reported for tissue-level AF specimens in the literature (Acaroglu et al., 1995; Ebara et al., 1996; Han et al., 2012; Werbner et al., 2019). Additionally, the notch geometry employed in this study reduced specimen cross-sectional area beyond those typically applied, which may also have resulted in higher apparent modulus values (Adams and Green 1993; Werbner et al., 2017). An additional limitation of this study is that only circumferential-axially oriented specimens were tested to maximize the contribution of collagen fibers (the constituent targeted by the applied disease-model) to the mechanical response.

This study sought to determine the relationship between AF advanced glycation end-product content and pre-failure, failure, and post-failure tensile mechanics at the tissue-level at two distinct loading rates. This was accomplished using an *in vitro* glycation treatment that induced two distinct, physiological AGE levels while maintaining hydration levels comparable to fresh tissue. We observed an increase in modulus, strength, and post-failure energy absorption capacity with increasing levels of glycation at both loading rates. AGE contents from a cross-sectional population of human cadaver discs were also presented. Results from this study may be used in development of advanced computational models that aim to study disc disease progression and to provide a deeper understanding of altered structure-function relationships that may lead to tissue dysfunction and failure (Zhou et al., 2019).

CRediT authorship contribution statement

Benjamin Werbner: Writing – review & editing, Writing – original draft, Visualization, Project administration, Methodology, Investigation, Formal analysis, Data curation, Conceptualization. Matthew Lee: Methodology, Writing – review & editing, Investigation. Allan Lee: Writing – review & editing, Methodology, Investigation. Linda Yang: Investigation, Methodology. Mohamed Habib: Investigation. Aaron J. Fields: Conceptualization, Funding acquisition, Investigation, Resources, Supervision, Writing – review & editing. Grace D. O'Connell: Writing – review & editing, Supervision, Resources, Methodology, Investigation, Funding acquisition, Conceptualization.

Declaration of competing interest

The authors declare that they have no known competing financial interests or personal relationships that could have appeared to influence the work reported in this paper.

Acknowledgements

The work was supported by the National Science Foundation (BMMB 1760467) and by the National Institutes of Health (R01 AR070198).

References

- Acaroglu, E.R., Latridis, J.C., Setton, L.A., Foster, R.J., Mow, V.C., Weidenbaum, M., 1995 Dec. Degeneration and aging affect the tensile behavior of human lumbar annulus fibrosus. Spine 1520 (24), 2690–2701.
- Acevedo, C., Sylvia, M., Schaible, E., Graham, J.L., Stanhope, K.L., Metz, L.N., Gludovatz, B., Schwartz, A.V., Ritchie, R.O., Alliston, T.N., Havel, P.J., 2018. Contributions of material properties and structure to increased bone fragility for a given bone mass in the UCD-T2DM rat model of type 2 diabetes. J. Bone Miner. Res. 33 (6), 1066–1075.
- Adams, M.A., Green, T.P., 1993. Tensile properties of the annulus fibrosus. Eur. Spine J. 2 (4), 203–208.
- Adams, M.A., Roughley, P.J., 2006. What is intervertebral disc degeneration, and what causes it? Spine 31 (18), 2151–2161.
- Ahmed, N., 2005. Advanced glycation endproducts—role in pathology of diabetic complications. Diabetes Res. Clin. Pract. 67 (1), 3–21.

- Allen, M.R., Newman, C.L., Chen, N., Granke, M., Nyman, J.S., Moe, S.M., 2015. Changes in skeletal collagen cross-links and matrix hydration in high-and low-turnover chronic kidney disease. Osteoporos. Int. 26 (3), 977–985.
- Andriotis, O.G., Elsayad, K., Smart, D.E., Nalbach, M., Davies, D.E., Thurner, P.J., 2019. Hydration and nanomechanical changes in collagen fibrils bearing advanced glycation end-products. Biomed. Opt Express 10 (4), 1841–1855.
- Bálint, G., Than, P., Domán, I., Wiegand, N., Horváth, G., Lőrinczy, D., 2009.
 Calorimetric examination of the human meniscus. J. Therm. Anal. Calorim. 95 (3), 759-761
- Beckstein, J.C., Sen, S., Schaer, T.P., Vresilovic, E.J., Elliott, D.M., 2008. Comparison of animal discs used in disc research to human lumbar disc: axial compression mechanics and glycosaminoglycan content. Spine 33 (6), E166–E173.
- Bezci, S.E., Nandy, A., O'Connell, G.D., 2015. Effect of hydration on healthy intervertebral disk mechanical stiffness. J. Biomech. Eng. 137 (10).
- Bezci, S.E., Torres, K., Carraro, C., Chiavacci, D., Werbner, B., Lim, S., O'Connell, G.D., 2020. Transient swelling behavior of the bovine caudal disc. J. Mech. Behav. Biomed. Mater. 112, 104089.
- Bezci, S.E., Werbner, B., Zhou, M., Malollari, K.G., Dorlhiac, G., Carraro, C., Streets, A., O'Connell, G.D., 2019. Radial variation in biochemical composition of the bovine caudal intervertebral disc. JOR Spine 2 (3), e1065.
- Bloom, E.T., Lee, A.H., Elliott, D.M., 2021. Tendon multiscale structure, mechanics, and damage are affected by osmolarity of bath solution. Ann. Biomed. Eng. 49 (3), 1058–1068.
- Buckwalter, J.A., 1995. Aging and degeneration of the human intervertebral disc. Spine 20 (11), 1307–1314.
- Centers for Disease Control and Prevention, 2020. National Diabetes Statistics Report.

 Centers for Disease Control and Prevention, U.S. Dept of Health and Human Services, 2020. Atlanta, GA.
- Chae, Y., Protsenko, D., Lavernia, E., Wong, B., 2009 Mar 1. Effect of water content on enthalpic relaxations in porcine septal cartilage. J. Therm. Anal. Calorim. 95 (3), 937–943.
- de Oliveira, R.R., de Lira, K.D., de Castro Silveira, P.V., Coutinho, M.P., Medeiros, M.N., Teixeira, M.F., de Moraes, S.R., 2011 May. Mechanical properties of achilles tendon in rats induced to experimental diabetes. Ann. Biomed. Eng. 39 (5), 1528–1534.
- Demers, C.N., Antoniou, J., Mwale, F., 2004 Dec 15. Value and limitations of using the bovine tail as a model for the human lumbar spine. Spine 29 (24), 2793–2799.
- Dolor, A., Sampson, S.L., Lazar, A.A., Lotz, J.C., Szoka, F.C., Fields, A.J., 2019 Apr 10. Matrix modification for enhancing the transport properties of the human cartilage endplate to improve disc nutrition. PLoS One 14 (4), e0215218.
- Domán, I., Illés, T., 2004 Oct 29. Thermal analysis of the human intervertebral disc. J. Biochem. Biophys. Methods 61 (1–2), 207–214.
- Ebara, S, Iatridis, J.C., Setton, L.A., Foster, R.J., Mow, V.C., Weidenbaum, M., 1996.
 Tensile properties of nondegenerate human lumbar anulus fibrosus. Spine 21 (4), 452–461.
- Fields, A.J., Berg-Johansen, B., Metz, L.N., Miller, S., La, B., Liebenberg, E.C., Coughlin, D.G., Graham, J.L., Stanhope, K.L., Havel, P.J., Lotz, J.C., 2015 May. Alterations in intervertebral disc composition, matrix homeostasis and biomechanical behavior in the UCD-T2DM rat model of type 2 diabetes. J. Orthop. Res. 33 (5), 738-746.
- Fox, A.J., Bedi, A., Deng, X.H., Ying, L., Harris, P.E., Warren, R.F., Rodeo, S.A., 2011 Jun. Diabetes mellitus alters the mechanical properties of the native tendon in an experimental rat model. J. Orthop. Res. 29 (6), 880–885.
- Freedman, M.K., Hilibrand, A.S., Blood, E.A., Zhao, W., Albert, T.J., Vacarro, A., Oleson, C.V., Morgan, T.S., Weinstein, J.N., 2011 Feb 15. The impact of diabetes on the outcomes of surgical and nonsurgical treatment of patients in the spine patient outcomes research trial. Spine 36 (4), 290.
- Gautieri, A., Passini, F.S., Silván, U., Guizar-Sicairos, M., Carimati, G., Volpi, P., Moretti, M., Schoenhuber, H., Redaelli, A., Berli, M., Snedeker, J.G., 2017 May 1. Advanced glycation end-products: mechanics of aged collagen from molecule to tissue. Matrix Biol. 59, 95–108.
- Gregory, D.E., Callaghan, J.P., 2010 Sep 1. An examination of the influence of strain rate on subfailure mechanical properties of the AF. J. Biomech. Eng. (9), 132.
- Guerin, H.L., Elliott, D.M., 2007 Apr. Quantifying the contributions of structure to AF mechanical function using a nonlinear, anisotropic, hyperelastic model. J. Orthop. Res. 25 (4), 508–516.
- Han, W.M., Nerurkar, N.L., Smith, L.J., Jacobs, N.T., Mauck, R.L., Elliott, D.M., 2012 Jul. Multi-scale structural and tensile mechanical response of AF to osmotic loading. Ann. Biomed. Eng. 40 (7), 1610–1621.
- Hollander, A.P., Heathfield, T.F., Webber, C., Iwata, Y., Bourne, R., Rorabeck, C., Poole, A.R., 1994 Apr. Increased damage to type II collagen in osteoarthritic articular cartilage detected by a new immunoassay. J. Clin. Investig. 193 (4), 1722–1732.
- Hoy, R.C., D'Erminio, D.N., Krishnamoorthy, D., Natelson, D.M., Laudier, D.M., Illien-Jünger, S., Iatridis, J.C., 2020 Sep 21. Advanced glycation end products cause RAGE-dependent AF collagen disruption and loss identified using in situ second harmonic generation imaging in mice intervertebral disk in vivo and in organ culture models. JOR Spine e1126.
- Illien-Jünger, S., Lu, Y., Qureshi, S.A., Hecht, A.C., Cai, W., Vlassara, H., Striker, G.E., latridis, J.C., 2015 Feb 10. Chronic ingestion of advanced glycation end products induces degenerative spinal changes and hypertrophy in aging pre-diabetic mice. PLoS One 10 (2), e0116625.
- Illien-Jünger, S., Torre, O.M., Kindschuh, W.F., Chen, X., Laudier, D.M., Iatridis, J.G., 2016 Nov 18. AGEs induce ectopic endochondral ossification in intervertebral discs. Eur. Cell. Mater. 32, 257.

- Isaacs, J.L., Vresilovic, E., Sarkar, S., Marcolongo, M., 2014 Dec 1. Role of biomolecules on AF micromechanics: effect of enzymatic digestion on elastic and failure properties. J. Mech. Behav. Biomed. Mater. 40, 75–84.
- Jazini, E., Sharan, A.D., Morse, L.J., Dyke, J.P., Aronowitz, E.A., Chen, L.K., Tang, S.Y., 2012 Feb 15. Alterations in magnetic resonance imaging T2 relaxation times of the ovine intervertebral disc due to non-enzymatic glycation. Spine 37 (4), E209.
- Jhawar, B.S., Fuchs, C.S., Colditz, G.A., Stampfer, M.J., 2006 Nov 1. Cardiovascular risk factors for physician-diagnosed lumbar disc herniation. Spine J. 6 (6), 684–691.
- Krishnamoorthy, D., Hoy, R.C., Natelson, D.M., Torre, O.M., Laudier, D.M., Iatridis, J.C., Illien-Jünger, S., 2018 Dec 1. Dietary advanced glycation end-product consumption leads to mechanical stiffening of murine intervertebral discs. Disease Models & Mechan. 11 (12).
- Li, Y., Fessel, G., Georgiadis, M., Snedeker, J.G., 2013 Apr 24. Advanced glycation endproducts diminish tendon collagen fiber sliding. Matrix Biol. 32 (3-4), 169–177.
- Licciardone, J.C., Kearns, C.M., Hodge, L.M., Minotti, D.E., 2013 Jun 1. Osteopathic manual treatment in patients with diabetes mellitus and comorbid chronic low back pain: subgroup results from the OSTEOPATHIC Trial. J. Am. Osteopath. Assoc. 113 (6), 468–478.
- Luoma, K., Riihimäki, H., Luukkonen, R., Raininko, R., Viikari-Juntura, E., Lamminen, A., 2000 Feb 15. Low back pain in relation to lumbar disc degeneration. Spine 25 (4), 487–492.
- Mäntyselkä, P., Miettola, J., Niskanen, L., Kumpusalo, E., 2008 Jun 30. Chronic pain, impaired glucose tolerance and diabetes: a community-based study. Pain 137 (1), 34-40.
- Monnier, V.M., Vishwanath, V., Frank, K.E., Elmets, C.A., Dauchot, P., Kohn, R.R., 1986 Feb 13. Relation between complications of type I diabetes mellitus and collagenlinked fluorescence. N. Engl. J. Med. 314 (7), 403–408.
- O'Connell, G.D., Guerin, H.L., Elliott, D.M., 2009 Nov 1. Theoretical and uniaxial experimental evaluation of human annulus fibrosus degeneration. J. Biomech. Eng. (11), 131.
- O'Connell, G.D., Leach, J.K., Klineberg, E.O., 2015 Nov 1. Tissue engineering a biological repair strategy for lumbar disc herniation. BioResearch Open Access 4 (1), 431–445.
- O'Connell, G.D., Vresilovic, E.J., Elliott, D.M., 2007 Feb 1. Comparison of animals used in disc research to human lumbar disc geometry. Spine 32 (3), 328–333.
- Pokharna, H.K., Phillips, F.M., 1998 Aug 1. Collagen crosslinks in human lumbar intervertebral disc aging. Spine 23 (15), 1645–1648.
- Reddy, G.K., Stehno-Bittel, L., Enwemeka, C.S., 2002 Mar 15. Glycation-induced matrix stability in the rabbit achilles tendon. Arch. Biochem. Biophys. 399 (2), 174–180.
- Reddy, G.K., 2004 Apr 1. Cross-linking in collagen by nonenzymatic glycation increases the matrix stiffness in rabbit achilles tendon. Exp. Diabesity Res. 5 (2), 143–153.
- Safa, B.N., Meadows, K.D., Szczesny, S.E., Elliott, D.M., 2017 Aug 16. Exposure to buffer solution alters tendon hydration and mechanics. J. Biomech. 61, 18–25.
- Samouillan, V., Delaunay, F., Dandurand, J., Merbahi, N., Gardou, J.P., Yousfi, M., Gandaglia, A., Spina, M., Lacabanne, C., 2011 Sep. The use of thermal techniques for the characterization and selection of natural biomaterials. J. Funct. Biomater. 2 (3), 230–248.
- Schmidt, H., Shirazi-Adl, A., Schilling, C., Dreischarf, M., 2016 Jun 14. Preload substantially influences the intervertebral disc stiffness in loading–unloading cycles of compression. J. Biomech. 49 (9), 1926–1932.
- Showalter, B.L., Beckstein, J.C., Martin, J.T., Beattie, E.E., Orías, A.A., Schaer, T.P., Vresilovic, E.J., Elliott, D.M., 2012 Jul 1. Comparison of animal discs used in disc research to human lumbar disc: torsion mechanics and collagen content. Spine 37 (15), E900
- Singh, R., Barden, A., Mori, T., Beilin, L., 2001 Feb. Advanced glycation end-products: a review. Diabetologia 44 (2), 129–146.
- Sivan, S.S., Tsitron, E., Wachtel, E., Roughley, P., Sakkee, N., Van Der Ham, F., Degroot, J., Maroudas, A., 2006 Oct 1. Age-related accumulation of pentosidine in

- aggrecan and collagen from normal and degenerate human intervertebral discs. Biochem. J. 399 (1), 29–35.
- Snedeker, J.G., Gautieri, A., 2014 Jul. The role of collagen crosslinks in ageing and diabetes-the good, the bad, and the ugly. Muscles, Ligaments Tendons J. 4 (3), 303.
- Stegemann, H., Stalder, K., 1967 Nov 1. Determination of hydroxyproline. Clin. Chim. Acta 18 (2), 267–273.
- Svensson, R.B., Mulder, H., Kovanen, V., Magnusson, S.P., 2013 Jun 4. Fracture mechanics of collagen fibrils: influence of natural cross-links. Biophys. J. 104 (11), 2476–2484
- Svensson, R.B., Smith, S.T., Moyer, P.J., Magnusson, S.P., 2018 Apr 1. Effects of maturation and advanced glycation on tensile mechanics of collagen fibrils from rat tail and Achilles tendons. Acta Biomater. 70, 270–280.
- Takahashi, S., Suzuki, A., Toyoda, H., Terai, H., Dohzono, S., Yamada, K., Matsumoto, T., Yasuda, H., Tsukiyama, K., Shinohara, Y., Ibrahim, M., 2013 Mar 15. Characteristics of diabetes associated with poor improvements in clinical outcomes after lumbar spine surgery. Spine 38 (6), 516–522.
- Tavakoli, J., Amin, D.B., Freeman, B.J., Costi, J.J., 2018 Sep. The biomechanics of the inter-lamellar matrix and the lamellae during progression to lumbar disc herniation: which is the weakest structure? Ann. Biomed. Eng. 46 (9), 1280–1291.
- Taylor, D., O'Mara, N., Ryan, E., Takaza, M., Simms, C., 2012 Feb 1. The fracture toughness of soft tissues. J. Mech. Behav. Biomed. Mater. 6, 139–147.
- Tsai, T.T., Ho, N.Y., Lin, Y.T., Lai, P.L., Fu, T.S., Niu, C.C., Chen, L.H., Chen, W.J., Pang, J.H., 2014 Feb. Advanced glycation end products in degenerative nucleus pulposus with diabetes. J. Orthop. Res. 32 (2), 238–244.
- Urban, J.P., Roberts, S., 2003 Jun. Degeneration of the intervertebral disc. Arthritis Res. Ther. 5 (3), 1, 1.
- Verzijl, N., DeGroot, J., Zaken, C.B., Braun-Benjamin, O., Maroudas, A., Bank, R.A., Mizrahi, J., Schalkwijk, C.G., Thorpe, S.R., Baynes, J.W., Bijlsma, J.W., 2002 Jan. Crosslinking by advanced glycation end products increases the stiffness of the collagen network in human articular cartilage: a possible mechanism through which age is a risk factor for osteoarthritis. Arthritis Rheum. 46 (1), 114–123.
- Viguet-Carrin, S., Roux, J.P., Arlot, M.E., Merabet, Z., Leeming, D.J., Byrjalsen, I., Delmas, P.D., Bouxsein, M.L., 2006 Nov 1. Contribution of the advanced glycation end product pentosidine and of maturation of type I collagen to compressive biomechanical properties of human lumbar vertebrae. Bone 39 (5), 1073–1079.
- Vlassara, H., Palace, M.R., 2002 Feb. Diabetes and advanced glycation endproducts. J. Intern. Med. 251 (2), 87–101.
- Von Forell, G.A., Hyoung, P.S., Bowden, A.E., 2014 Jul 1. Failure modes and fracture toughness in partially torn ligaments and tendons. J. Mech. Behav. Biomed. Mater. 35, 77–84.
- Wagner, D.R., Reiser, K.M., Lotz, J.C., 2006 Jan 1. Glycation increases human AF stiffness in both experimental measurements and theoretical predictions. J. Biomech. 39 (6), 1021–1029.
- Werbner, B., Zhou, M., McMindes, N., Lee, A., Lee, M., O'Connell, G.D., 2021 Nov 2. Saline-polyethylene glycol blends preserve in vitro annulus fibrosus hydration and mechanics: an experimental and finite-element analysis. J. Mech. Behav. Biomed. Mater. 104951.
- Werbner, B., Spack, K., O'Connell, G.D., 2019 May 24. Bovine AF hydration affects rate-dependent failure mechanics in tension. J. Biomech. 89, 34–39.
- Werbner, B., Zhou, M., O'Connell, G.D., 2017 Nov 1. A novel method for repeatable failure testing of AF. J. Biomech. Eng. 139 (11).
- White III, A.A., Panjabi, M.M., 1990. Clinical Biomechanics of the Spine.
- Zhou, M., Bezci, S.E., O'Connell, G.D., 2019 Nov 4. Multiscale composite model of fiber-reinforced tissues with direct representation of sub-tissue properties. Biomech. Model. Mechanobiol. 1–5.
- Zhou, M., Lim, S., O'Connell, G.D., 2021. A robust multiscale and multiphasic structure-based modeling framework for the intervertebral disc. Front. Bioeng. Biotechnol. 9, 685799